

Identification of Catalytic Cysteine, Histidine, and Lysine Residues in *Escherichia coli* Homoserine Transsuccinylase[†]

Katharine Ziegler,[‡] Schroeder M. Noble,[§] Elissa Mutumanje,[‡] Barney Bishop,[‡] Donald P. Huddler,[§] and Timothy L. Born^{*,‡}

Department of Chemistry & Biochemistry, George Mason University, 10900 University Boulevard, Manassas, Virginia 20110, and Division of Experimental Therapeutics, Walter Reed Army Institute of Research, 503 Robert Grant Avenue, Silver Spring, Maryland 20910

Received September 28, 2006; Revised Manuscript Received December 15, 2006

ABSTRACT: Homoserine transsuccinylase catalyzes the succinylation of homoserine in several bacterial species, the first unique step in methionine biosynthesis in these organisms. The enzyme from *Escherichia coli* is reported to be a dimer and uses a ping-pong catalytic mechanism involving transfer of succinate from succinyl-CoA to an enzyme nucleophile, followed by transfer to homoserine to form *O*-succinylhomoserine. Site-directed mutagenesis and steady-state kinetics were used to identify three amino acids that participate in catalysis. Mutation of cysteine-142 to serine or alanine eliminated all measurable activity, suggesting this amino acid acts as the catalytic nucleophile. Cysteine nucleophiles are often deprotonated by histidine residues, and histidine-235 was identified as the sole absolutely conserved histidine residue among family members. This residue was mutated to both alanine and asparagine, and no activity was observed with either mutant. Lysine-47 had been previously identified as an essential residue. Mutation of this amino acid to arginine reduced catalytic activity by greater than 90%, while mutation to alanine yielded an enzyme with <1% of wild-type activity. A pH–rate profile of the K47R mutant demonstrated that this amino acid participates in the first half reaction. The data presented here provide the first detailed description of the homoserine transsuccinylase active site and provide a framework for additional mechanistic characterization of this enzyme.

Methionine is one of 10 essential dietary amino acids. Both microorganisms and plants synthesize methionine from aspartate, and methionine and its derivatives *S*-adenosylmethionine (SAM)¹ and acylhomoserine lactones (HSLs) are essential compounds that fill numerous biological roles. For example, methionine is one of the basic building blocks of proteins and is the initiating amino acid in protein biosynthesis, while SAM is a cofactor used to transfer reduced C₁ fragments in methylation reactions. SAM is also the source of propylamine groups found in spermidine and spermine (1). HSLs are signaling molecules synthesized from SAM

by Gram-negative bacteria, which are used to monitor cell density in a phenomenon known as quorum sensing (2). Although humans do not synthesize methionine, they can interconvert methionine and cysteine via the transsulfuration pathway (3). Mutations or deletions of enzymes involved in methionine biochemistry lead to various metabolic defects in humans (4), and inhibition of methionine biosynthesis in microorganisms leads to the arrest of cell growth (5). These properties make enzymes in the methionine biosynthetic pathway attractive targets for the design of novel inhibitors.

Homoserine is the last common precursor in the biosynthetic pathways of methionine, threonine, and isoleucine (Figure 1). The conversion of homoserine to methionine by microorganisms and plants can occur by one of two routes. The first route occurs primarily in microorganisms and involves acylation of homoserine. In *Escherichia coli*, the committed step in the pathway is the succinylation of homoserine to form *O*-succinylhomoserine, while homoserine is acetylated to form *O*-acetylhomoserine in *Haemophilus influenzae* (6). Succinylation is catalyzed by the *metA*-encoded homoserine transsuccinylase (HTS) and acetylation by the *met2*-encoded homoserine transacetylase (HTA). Acylation of homoserine presumably provides the free-energy input necessary to commit homoserine to methionine biosynthesis and prepares the γ -hydroxyl for subsequent condensation with cysteine to form cystathionine, a reaction catalyzed by the *metB* gene product. Cleavage of cystathionine by *metC* yields homocysteine, which is methylated to

[†]This work was supported in part by the National Institutes of Health (GM064513 to T.L.B.) and by the Undergraduate Research Apprenticeship program at George Mason University (to E.M.). Acknowledgement is made to the donors of The Petroleum Research Fund, administered by the ACS, for partial support of this research. S.M.N. and D.P.H. are supported by a Defense Threat Reduction Agency grant.

* To whom correspondence should be addressed: E-mail: tborn@gmu.edu. Phone: 703-993-4171. Fax: 703-993-9575.

[‡] George Mason University.

[§] Walter Reed Army Institute of Research.

¹ Abbreviations: BcHTS, *Bacillus cereus* homoserine transsuccinylase; CoA, coenzyme A; DEPC, diethylpyrocarbonate; EcHTS, *Escherichia coli* homoserine transsuccinylase; HiHTA, *Haemophilus influenzae* homoserine transacetylase; HSL, acylhomoserine lactone; HTA, homoserine transacetylase; HTS, homoserine transsuccinylase; IAA, iodoacetamide; IPTG, isopropyl- β -D-thiogalactopyranoside; OAH, *O*-acetylhomoserine; OSH, *O*-succinylhomoserine; PLP, pyridoxal phosphate; SAM, *S*-adenosylmethionine; SDS–PAGE, sodium dodecyl sulfate–polyacrylamide gel electrophoresis; TEA, triethanolamine; TmHTS, *Thermotoga maritima* homoserine transsuccinylase.

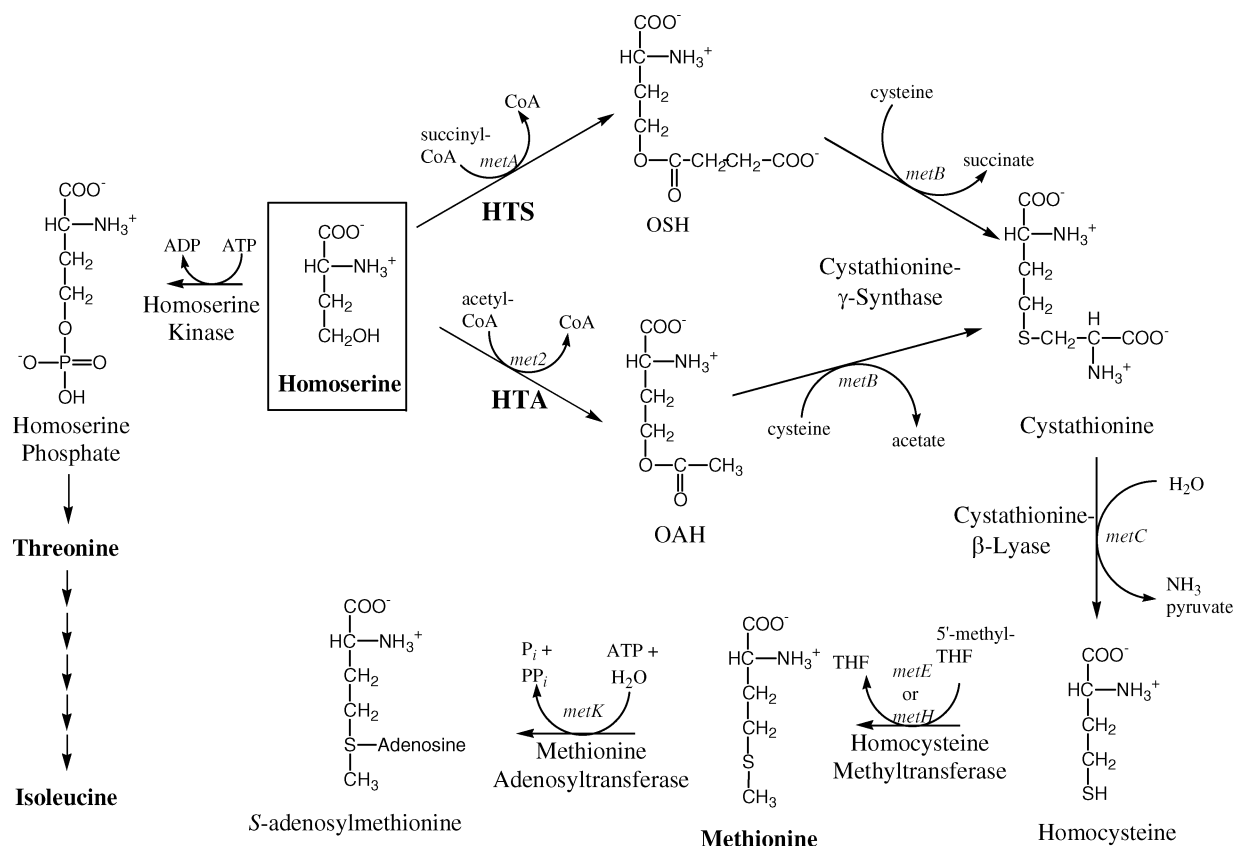


FIGURE 1: Biosynthetic pathways in *E. coli* of methionine and S-adenosylmethionine. Gene and enzyme names are indicated above the arrows, and structures of the primary intermediates are included. Additional amino acids derived from homoserine are indicated.

produce methionine via either a vitamin B₁₂-dependent (*metH*) or -independent (*metE*) homocysteine methylase. Methionine can then be adenylylated by methionine adenosyltransferase (*metK*) to form SAM. SAM, in turn, is utilized by the LuxI family of proteins to synthesize HSLs (7). It is interesting to note that two steps in the bacterial methionine biosynthetic pathway can be catalyzed by multiple enzymes. The second route of methionine biosynthesis occurs primarily in plants. In this pathway, homoserine is activated via phosphorylation and is then directly sulfhydrylated by H₂S to form homocysteine, which is converted to methionine as described above.

Homoserine transsuccinylase (EC 2.1.3.46) is found in a variety of microorganisms, including human pathogens such as *Yersinia pestis*, *Bacillus anthracis*, *Salmonella typhimurium*, and *Streptococcus pneumoniae*. HTS catalyzes the transfer of succinate from succinyl-CoA to homoserine via a ping-pong kinetic mechanism. In the first half reaction, an enzyme nucleophile accepts succinate from succinyl-CoA, forming a succinylated enzyme and releasing CoA. In the second half reaction, L-homoserine binds to the enzyme, succinate is transferred from the enzyme nucleophile to the γ-hydroxyl group of homoserine, and O-succinylhomoserine is released, preparing the enzyme for a second round of catalysis (8).

Iodoacetamide inactivates the enzyme in a pH- and concentration-dependent manner, suggesting that a cysteine residue may be involved in the catalytic mechanism as the nucleophile for succinylation or that it may be required for maintenance of the active structure (8). A recent study used mass spectrometry to identify two succinylated lysine

residues, and the authors suggested that lysine acts as the catalytic nucleophile (9). Little else is known about residues involved in catalysis, and confusion exists regarding the catalytic nucleophile, prompting a more in-depth study of *E. coli* HTS (EcHTS) catalytic residues.

In this study, we identified three active site residues of EcHTS through the use of site-directed mutagenesis and steady-state kinetics. Cysteine-142 was identified as the active site nucleophile, while histidine-235 is proposed to be the active site base responsible for deprotonation of this cysteine residue. Furthermore, it is demonstrated that the primary role of lysine-47 is not as a nucleophile, but this residue plays an unspecified role in the first half of the ping-pong reaction. A model of the enzymatic mechanism that incorporates these data and recent structural evidence is proposed.

MATERIALS AND METHODS

Materials. Oligonucleotide primers used for PCR amplification were synthesized by Invitrogen Custom Primers (Carlsbad, CA). The pET23a expression vector, *E. coli* BL21 (DE3) cells, and *E. coli* Rosetta 2(DE3) cells were purchased from Novagen (Madison, WI). *E. coli* genomic DNA was purchased from ATCC (Manassas, VA), and DNaseI was from Epicenter (Madison, WI). IPTG was purchased from Calbiochem (San Diego, CA), and chromatographic supports for protein purification were from GE Healthcare Life Sciences (Piscataway, NJ). All other chemicals were purchased from Sigma-Aldrich Chemical Co. (St. Louis, MO). DNA sequencing was performed by Northwoods DNA, Inc (Bemidji, MN).

Generation of *E. coli* Homoserine Transsuccinylase mutants. The gene for EcHTS (*metA*) had previously been cloned into the pET23a expression vector (8). Oligonucleotide primers encoding for select single and double mutants were synthesized and used to create the desired *E. coli* *metA* mutant in the pET23a expression vector using the QuikChange Site-Directed Mutagenesis kit (Stratagene) by following the manufacturer's protocol. The K46A and K46R plasmid DNAs were used as templates for the generation of the K46A/K47A and K46R/K47R double mutants. Recombinant plasmids were transformed into competent *E. coli* BL21 (DE3) or *E. coli* Rosetta 2(DE3) cells, which were then used to express the protein under IPTG induction. Analysis by SDS-PAGE with Coomassie blue staining indicated the overexpression of a 35–40 kDa soluble protein with each mutant.

Protein Purification. The general procedure for protein purification involved inoculation of LB containing ampicillin (50 mg/L) with a bacterial colony. The cultures were grown to an OD₆₀₀ of 0.5–0.7 before induction with 0.5 mM IPTG. Cells were grown for a minimum of 3 h following induction before harvesting by centrifugation and resuspension in 25 mM triethanolamine (TEA, pH 7.8). All subsequent steps were performed at 4 °C. Cell lysis was initiated by the addition of lysozyme (0.2 mg/mL) in the presence of 10 mM MgCl₂ and DNaseI and the solution was stirred for 30 min. The cells were fully lysed by sonication and the cell debris was removed by centrifugation at 12000g for 1 h. The supernatant was dialyzed against two changes of dialysis buffer (4 L; 25 mM TEA (pH 7.8), 25 mM NaCl). Insoluble matter was removed by centrifugation at 12000g for 30 min before loading the supernatant onto a fast-flow Q-Sepharose anion-exchange column (26 × 2.6 cm) that had been equilibrated with 25 mM TEA (pH 7.8). The protein was eluted at a rate of 1 mL/min with a 450 mL linear 0 to 1 M NaCl gradient. The fractions containing active protein were pooled, and solid (NH₄)₂SO₄ was added to a final concentration of 1 M. Any precipitate that formed was removed by centrifugation prior to loading the supernatant onto a Phenyl-Sepharose column (30 × 1.6 cm) that had been equilibrated with 1 M (NH₄)₂SO₄ in 25 mM TEA (pH 7.8). The protein was eluted at a rate of 0.5 mL/min with a 250 mL linear 1 to 0 M (NH₄)₂SO₄ gradient. The active fractions, which were >90% pure according to SDS-PAGE analysis, were pooled and dialyzed against 4 L of 25 mM TEA (pH 7.8). Following dialysis, the purified protein was concentrated and stored at –20 °C in 50% glycerol or in 25 mM TEA (pH 7.8) containing 500 mM NaCl. Four mutants (C142A, K47A, K46R/K47R, and K46A/K47A) precipitated in the presence of 1 M ammonium sulfate. In these cases, the precipitate was collected by centrifugation, resuspended in 25 mM TEA (pH 7.8), and dialyzed to reduce the ammonium sulfate concentration to less than 100 μM. The precipitated mutants were determined to be pure via SDS-PAGE and stored as mentioned above.

Measurement of Enzyme Activity. Reaction rates were determined by monitoring the decrease in absorbance at 232 nm due to hydrolysis of the thioester bond of succinyl-CoA ($\epsilon = 4500 \text{ M}^{-1}$) in a UVIKON 933 double beam UV/vis spectrophotometer (Research Instruments International). Assays were performed in 50 mM KH₂PO₄ (pH 7.2) at 25 °C. Reactions were initiated by the addition of enzyme, and initial

velocity kinetic data were fit to eq 1 using the program SigmaPlot (version 7.101):

$$v = V_{\text{AB}}/(K_{\text{A}}[\text{B}] + K_{\text{B}}[\text{A}] + [\text{A}][\text{B}]) \quad (1)$$

where V is the maximal velocity, A and B are the concentrations of substrates A and B , respectively, and K_{A} and K_{B} are the Michaelis constants for substrates A and B , respectively. Initial velocities were determined at 25 unique combinations of five succinyl-CoA concentrations and five L-homoserine concentrations.

The stereospecificity of select mutants was analyzed with L- and D-homoserine. Initial velocities were determined at a minimum of seven different concentrations of L- and D-homoserine (0.5–2500 μM L-homoserine depending on the enzyme and 25 to 10000 μM D-homoserine depending on the enzyme) at a constant 100 μM concentration of succinyl-CoA. Initial velocity kinetic data were fit to eq 2 using SigmaPlot:

$$V_{\text{o}} = V_{\text{max}}[\text{S}]/(K_{\text{M}} + [\text{S}]) \quad (2)$$

where V_{o} is the initial velocity, V_{max} is the maximum velocity, $[\text{S}]$ is the homoserine concentration, and K_{M} is the Michaelis constant.

pH Profiles. Enzyme activity was measured over the pH range of 6.25–8.5 using phosphate buffer for the EcHTS K47R mutant and over the pH range of 6.25–7.2 for the EcHTS K46A mutant. Assays were performed at 25 °C in 50 mM buffer, and reactions were initiated by addition of enzyme. Initial velocities were determined at 25 unique combinations of five concentrations of succinyl-CoA (25, 50, 100, 150, and 200 μM) and five concentrations of L-homoserine (10, 25, 50, 100, and 150 μM). The kinetic values V_{max} and $V_{\text{max}}/K_{\text{M}}$ were determined and the data were fit to eq 3 using SigmaPlot:

$$\log V = \log[C/(1 + H/K_{\text{a}})] \quad (3)$$

where V is the maximal velocity (or $V_{\text{max}}/K_{\text{M}}$), C is the pH-independent plateau value, H is the hydrogen ion concentration, and K_{a} is the ionization constant for the acidic group.

Inactivation by Iodoacetamide. A solution containing 50 μg of EcHTS K47R in 100 mM phosphate buffer was inactivated at 25 °C by the addition of iodoacetamide to a final concentration of 75 μM (100 μL final volume). At various time points, 10 μL aliquots were removed and added to an assay solution containing 100 mM K₂HPO₄ (pH 7.1), 100 μM L-homoserine, and 100 μM succinyl-CoA in a final volume of 500 μL. The residual enzyme activity was measured by monitoring the change in absorbance at 232 nm. The rate of inactivation was measured over a pH range of 6.25–8.0 using phosphate buffer, and the data were fit to eq 3, substituting the rate of inactivation for the maximal velocity.

Diethylpyrocarbonate Inactivation. Diethylpyrocarbonate (DEPC) was used to chemically modify EcHTS histidine residues. The 100 μL inactivation mixture contained 25 μg of enzyme in 100 mM phosphate buffer (pH 7.5), to which different amounts of DEPC were added for each assay. Aliquots of 5 μL were taken from the inactivation mixture at various time points and added to an assay mixture containing 100 mM phosphate buffer (pH 7.5), 5 mM

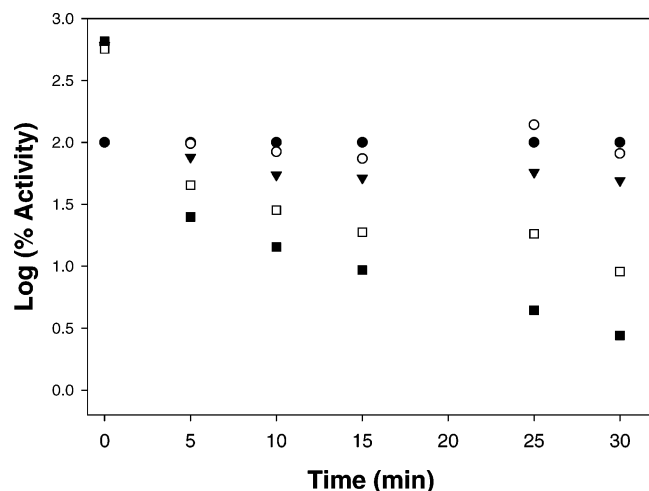


FIGURE 2: Inactivation of EcHTS by diethylpyrocarbonate. EcHTS was incubated with DEPC for varying periods of time, and the remaining activity was determined. The log(% activity), in comparison to a control reaction without DEPC, was then calculated at each time point, and the data were plotted. (●) 0 μ M DEPC; (○) 50 μ M DEPC; (▼) 100 μ M DEPC; (□) 150 μ M DEPC; (■) 250 μ M DEPC.

homoserine, and 200 μ M succinyl-CoA in a final volume of 500 μ L. Enzyme activity was then measured as described above, and the percent activity was determined at each time point by comparison to a control reaction that lacked DEPC.

Homology Modeling. Comparative models of EcHTS were developed with Modeller 8v2 using the experimental structures of *B. cereus* (2GHR) and *T. maritima* (2H2W) HTS as templates (10–12). In the *B. cereus* experimental structure (BcHTS), residues 74 through 87 are disordered and not present in the final structure deposited in the PDB. This segment of EcHTS was modeled based on the corresponding segment of the *T. maritima* experimental structure (TmHTS). PyMol (13) was used to examine the final, optimized models and to generate structural figures.

RESULTS

Chemical Modification of EcHTS and Generation of Mutants. It had previously been established that iodoacetamide inactivated EcHTS (8), suggesting the presence of a cysteine residue at the enzyme active site. Deprotonation of this cysteine is essential for its proposed role as a nucleophile, leading to the possibility that a cysteine–histidine pair might exist at the active site since this pairing is known to occur in other enzyme systems (14–16). The presence of an essential histidine residue was investigated via chemical modification of EcHTS by DEPC. Enzyme was incubated with DEPC at concentrations of 50, 100, 150, and 250 μ M, and aliquots containing 1.25 μ g of EcHTS were removed at varying time points. Initial velocities were then determined in the presence of 200 μ M succinyl-CoA and 5 mM homoserine, and the percent activity remaining was calculated in comparison to a control sample. As shown in Figure 2, DEPC inactivates EcHTS in a time-dependent fashion, and the rate of inactivation depends on the DEPC concentration, suggesting the presence of an active site histidine residue.

The identity of the catalytic cysteine and histidine residues was assessed via site-directed mutagenesis. EcHTS contains

two cysteine residues, at positions 90 and 142, with C142 absolutely conserved among all known HTS-like sequences and C90 often substituted by a wide variety of amino acids. Although C142 was presumed to be the catalytic nucleophile, both cysteine residues were mutated to alanine and to serine. The likely catalytic histidine residue was identified from an alignment of 100 HTS-like amino acid sequences. This alignment revealed a single conserved histidine residue, histidine-235, which was mutated to both asparagine and alanine. In addition to a cysteine–histidine catalytic pair, a recent report (9) suggested the involvement of one or two lysines in catalysis (K46 and K47). Both of these residues were individually mutated to arginine and alanine, and the double-alanine and double-arginine mutants were also created. All plasmid DNAs were sequenced to verify that the correct mutations had been incorporated.

EcHTS mutants were overexpressed in *E. coli* cells transformed with the appropriate plasmid, and protein production was induced with IPTG. After cell lysis, the EcHTS mutants were purified by anion exchange and hydrophobic affinity. SDS–PAGE analysis was used to identify fractions containing purified protein. Although the majority of the mutants in this study were soluble at the ammonium sulfate concentration used for hydrophobic chromatography, four mutants (C142A, K47A, K46R/K47R, and K46A/K47A) precipitated in a pure form in the presence of 1 M ammonium sulfate and were used after resolubilization and dialysis.

Determination of Mutant Steady-State Parameters. Enzyme activity was measured by monitoring the decrease in absorbance at 232 nm due to hydrolysis of the thioester bond of succinyl-CoA. Initial velocities for each mutant were determined at 25 unique combinations of five succinyl-CoA concentrations and five L-homoserine concentrations, and the data were fit to a ping-pong kinetic mechanism (eq 1) for determination of K_M and k_{cat} values. The resulting kinetic parameters are listed in Table 1. The limit of detectable activity for this assay corresponds to a k_{cat} of 0.05 s^{-1} , and thus any mutants listed as inactive in Table 1 may have a residual activity of this magnitude. As can be seen from the data, the K_M for succinyl-CoA is essentially constant for each of the active mutants, while the K_M for homoserine varies by a factor of ~ 300 .

The lack of measurable activity with the C142A and C142S mutants strongly suggests that this residue is involved in catalysis. This is further supported by the full activity of the C90S mutant and the high activity of the C90A mutant. Both of the H235 mutants were inactive, indicating that this residue plays an important role in catalysis or structure. It is likely that both H235A and H235N are properly folded since each mutant purified in an identical manner to the wild-type enzyme. It appears that both lysine-46 and lysine-47 are essential for maximal activity, but changes at position 47 are much more deleterious than changes at position 46. Lysine-47 is highly conserved, it is found in 88 of 100 HTS-like sequences, and this residue is more likely to be directly involved in catalysis or formation of an active enzyme conformation.

Because an effect was seen on the homoserine K_M values with the two lysine mutants, we tested whether either of these amino acids was responsible for the enzyme's stereospecificity for L-homoserine. Initial velocities were determined

Table 1: Summary of Mutant Kinetic Constants^a

enzyme	K_M succinyl-CoA (μM)	K_M L-homoserine (μM)	k_{cat} (s^{-1})	k_{cat}/K_M (succinyl-CoA) ($\text{s}^{-1}\text{M}^{-1}$)	k_{cat}/K_M (homoserine) ($\text{s}^{-1}\text{M}^{-1}$)
WT EcHTS	130 \pm 10	720 \pm 60	130 \pm 10	1.0×10^6	1.8×10^5
C90S	140 \pm 40	1070 \pm 350	130 \pm 20	9.3×10^5	1.2×10^5
K46R	130 \pm 20	580 \pm 70	37 \pm 3	2.8×10^5	6.4×10^4
K46A	140 \pm 30	44 \pm 10	4.1 \pm 0.6	2.9×10^4	9.3×10^4
K47R	94 \pm 14	49 \pm 6	1.8 \pm 0.1	1.9×10^4	3.7×10^4
K47A	160 \pm 30	3.2 \pm 1.1	0.34 \pm 0.04	2.1×10^3	1.1×10^5
K46RK47R	130 \pm 20	27 \pm 3	2.0 \pm 0.1	1.5×10^4	7.4×10^4
C142A ^b	inactive				
C142S ^b	inactive				
H235A ^b	inactive				
H235N ^b	inactive				
K46AK47A ^c	minimal activity				

^a Assays were performed at 25 °C in 50 mM KH₂PO₄, pH 7.2. ^b No activity could be detected with these mutants; the limit of detectable activity corresponds to a k_{cat} of 0.05 s⁻¹. ^c Although activity could be measured with this double mutant, it was not possible to accurately determine K_M or k_{cat} values.

at a minimum of seven different concentrations of L- and D-homoserine while holding the succinyl-CoA concentration constant at 100 μM . The K_M values of wild-type EcHTS and the K46A, K46R, and K47R mutants for the two stereoisomers of homoserine indicates that each prefers L-homoserine over D-homoserine by a factor of 10–20. The extremely low activity of the K47A mutant made it difficult to obtain accurate data, but it also had a clear preference for L-homoserine. Since each mutant has a similar preference as the wild-type enzyme for L-homoserine, these data suggest that K46 and K47 are not involved in determination of homoserine stereospecificity.

pH Profiles. The proposed mechanism for EcHTS involves the use of general acid and general base catalysis in each half reaction (8), suggesting a possible role for K47 that could be probed via pH studies. The activity of the K47R mutant was measured over the pH range of 6.25–8.5. As can be seen in Figure 3A, the pH dependence of the maximal velocity of K47R decreases as the pH is lowered, and a similar effect is seen on $V/K_{\text{succinyl-CoA}}$ (Figure 3B). Fitting of these data to eq 3 yielded a $\text{p}K_a$ value of 7.5 for each set, which is approximately one pH unit greater than those reported for the wild-type enzyme (8). In contrast, no pH dependence of $V/K_{\text{homoserine}}$ was observed for K47R in the pH range tested (Figure 3C), while the wild-type enzyme exhibited a loss of activity at lower pH and a $\text{p}K_a$ value of 6.5. The pH dependence of $V/K_{\text{homoserine}}$ for the K46A mutant was then studied to determine if the observations with K47R were unique to this mutant or if mutation of either lysine residue would yield the same results. The K46A mutant was chosen since it had kinetic properties similar to the K47R mutant. This mutant loses activity with decreasing pH, with a slope of 1 that is consistent with results for the wild-type enzyme. These experimental data suggest that only the lysine residue at position 47 is required for maximal catalysis.

IAA Inactivation. The shift in $\text{p}K_a$ values in the V_{max} and $V/K_{\text{succinyl-CoA}}$ profiles for the K47R mutant was unexpected since it had been previously concluded from iodoacetamide inactivation studies that this ionization reflected the catalytic cysteine residue. Therefore, the pH dependence of IAA inactivation was studied with the K47R mutant. The inactivation of EcHTS K47R by IAA was concentration- and time-dependent, and the rate of inactivation increased as the

pH was increased from 6.25, leveling off at the higher pH values examined (Figure 3D). A $\text{p}K_a$ value of 6.8 was determined from the data. This is more similar to the value of 6.4 measured for IAA inactivation of the wild-type enzyme than it is to the value of 7.5 measured in the V_{max} and $V/K_{\text{succinyl-CoA}}$ profiles of the K47R mutant.

DISCUSSION

The metabolite homoserine is a biosynthetic precursor of three amino acids. As such, its fate is tightly regulated. In *E. coli* the primary point of regulation is the enzyme homoserine transsuccinylase, which succinylates the hydroxyl group of homoserine and commits it to methionine biosynthesis. The amount of EcHTS activity in the cell is controlled at the genetic level by the MetJ repressor and the MetR activator (17). The enzyme also appears to be controlled by the heat shock response and its activity is highly sensitive to temperature (18, 19). In addition, EcHTS is feedback inhibited by both methionine and S-adenosylmethionine, the final products of the methionine biosynthetic pathway (20, 21). The basic mechanism of the enzyme has been outlined (8), and at least one active site amino acid has been proposed (9), but little is known about the specific identity of catalytic residues or their role in catalysis. In this paper, we describe the identification of three active site residues and propose roles for each residue in catalysis based on the data presented and recent structural information.

The presence of an active site cysteine residue was suggested in an earlier study (8), and this cysteine was proposed to function as the catalytic nucleophile. EcHTS contains two cysteine residues, at positions 90 and 142, either of which could theoretically participate in catalysis. From an alignment of 100 HTS-like sequences, it was observed that the cysteine residue at position 90 was substituted by a wide variety of residues in other organisms, making it unlikely that this residue was essential to catalysis. The results of experiments with two mutants at this position, C90A and C90S, are consistent with this conclusion as the activity of the C90S mutant was equivalent to that of the wild-type enzyme and the C90A mutant also retained substantial activity (although it was not quantified). The same alignment showed that C142 was absolutely conserved, and

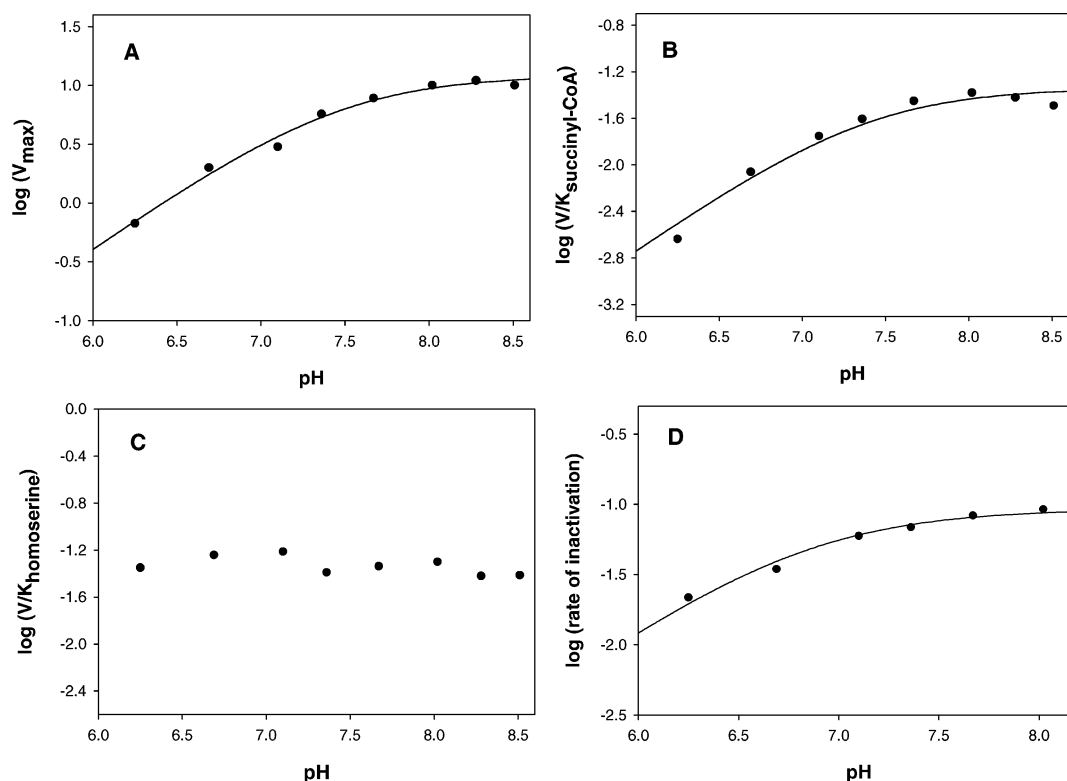


FIGURE 3: pH dependence of EcHTS lysine mutants and effect of pH on iodoacetamide inactivation. Experiments were conducted as described in Materials and Methods using phosphate buffer to adjust the pH. Symbols represent the experimental data obtained with EcHTS K47R, and the curves are fits of the data to eq 3. (A) Dependence of maximal velocity on pH. The units of maximal velocity are micromoles per minute per milligram of protein. (B) Dependence of $V/K_{\text{succinyl-CoA}}$ on pH. The values of V are measured in units of maximal velocity, and $K_{\text{succinyl-CoA}}$ is in μM units. (C) Dependence of $V/K_{\text{homoserine}}$ on pH. The values of V are measured in units of maximal velocity, and $K_{\text{homoserine}}$ is in μM units. (D) Dependence of the rate of inactivation of EcHTS K47R by iodoacetamide on pH. The rate of inactivation is measured in units of remaining initial velocity (micromoles per minute per milligram) per minute.

it was observed that mutation of this residue had severe effects on enzyme activity. Both the C142A and the C142S mutants had no measurable activity, suggesting that this residue is essential to catalysis. The most likely role for C142 is that of a nucleophile that accepts a succinate group from succinyl-CoA before transferring that group to homoserine. Significant precedence for cysteine nucleophiles exists from the cysteine protease family of enzymes as well as from other enzyme families (14, 22–28).

For C142 to function as a nucleophile, it must be deprotonated by an active site base, a role that is filled by histidine in many cases (14–16). The presence of an essential histidine was confirmed by chemical modification experiments using diethylpyrocarbonate to alkylate histidine residues. This compound inhibited EcHTS in a time- and concentration-dependent manner, as would be expected for alkylation of an active site residue. Addition of succinyl-CoA to the inactivation mixture reduced the rate of inactivation, as would be expected for a chemical modification agent directed toward a residue located at the active site. Caution must be taken when interpreting modifications with DEPC, however, since this compound is known to modify tyrosine, lysine, and cysteine residues when used in large excess (29). Analysis of an HTS amino acid sequence alignment indicated the presence of a single histidine residue that was absolutely conserved (H235), and this residue was mutated to both alanine and asparagine in order to determine whether it played a role in catalysis. It was hoped that mutation to asparagine would allow retention of some residual activity

so that a specific role for H235 could be further explored while it was thought that mutation to alanine would abolish all activity. Both mutants had no measurable catalytic activity, however, suggesting that H235 is critical to catalysis. Chemical rescue experiments with the H235A mutant were unsuccessful. The lack of activity with both mutants makes it difficult to assign a specific role to this residue, although these data are consistent with a role as a general base required to deprotonate C142. The H235A mutant would be unable to function as a base, explaining the lack of activity with this protein. Mutation to asparagine should maintain some of the basic structure of the original histidine residue, but this amino acid would also be unlikely to act as a base. Hence, lack of activity with the H235N mutant is consistent with the proposal that this amino acid functions as a base during catalysis. Recent structural data provides further support for this proposal, as discussed in more detail below.

Rosen et al. (9) used 2D gel electrophoresis and mass spectrometry to identify a succinylated lysine residue in EcHTS and based on this information suggested that this residue is the active site nucleophile. Both lysine-46 and lysine-47 (these two lysines are referred to as lysine-45 and lysine-46 in the paper by Rosen et al.) were found to be succinylated, so it was not possible to conclusively assign the role of active site nucleophile to either residue, although it was noted that only K47 was conserved among an alignment of 12 HTS-like sequences. Further evidence for the importance of these residues was established by transforming *E. coli* cells lacking the *metA* gene with a plasmid

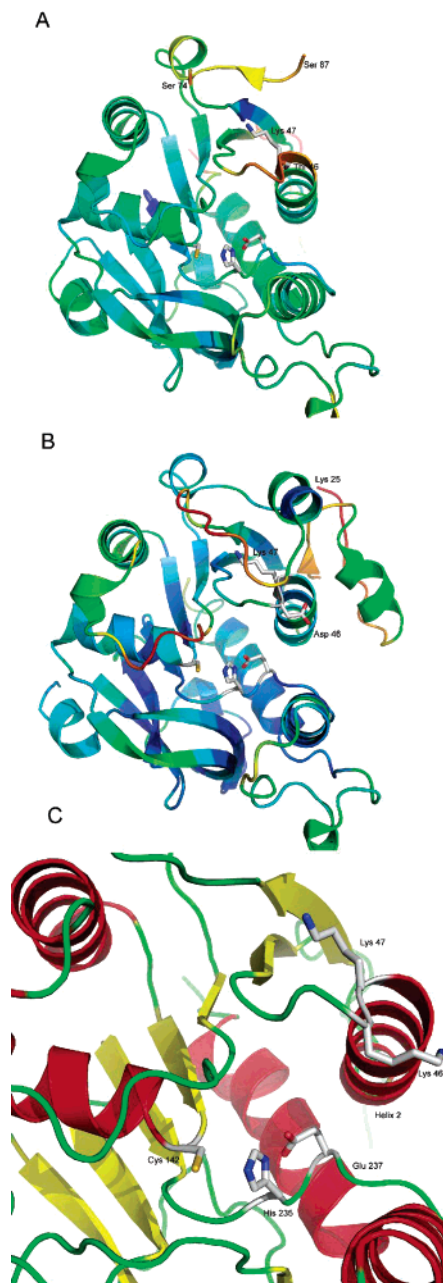


FIGURE 4: Structures of homoserine transsuccinylases. Ribbon diagram (A) of *B. cereus* HTS (2GHR, 2.4 Å). The loop residues (74–84) not observed in the experimental structure lie in a rather mobile segment of the structure. Portions of this mobile region may be responsible for binding substrates or possibly regulating substrate binding or product release through conformational changes. Panel B shows the same view of the *T. maritima* HTS structure (2H2W, 2.5 Å). As observed in BcHTS, residues 17–112 of TmHTS appear more mobile than the remainder of the structure. The loop region corresponding to 74–84 in BcHTS is observed in this structure and is among the most mobile segments in the model as judged by normalized B-factors. This observed mobility supports our hypothesis that the loop region may make conserved contacts between the D/K/T46K47 region and play a role in substrate binding, release, or regulation of binding or release. Panels A and B are colored based on B-factor, with blue indicating a stable structure and a small B-factor and red representing a highly flexible structure and a large B-factor. Panel C shows the active site region and surrounding secondary structure elements of our EcHTS homology model based on the experimental structures shown in A and B. This figure is colored based on secondary structure. Overall, we predict that the EcHTS experimental structure will closely resemble the BcHTS and TmHTS structures with differences in the region corresponding to 72–86 but possess similar flexibility and function.

encoding a mutant version of EcHTS where both lysines were converted to alanine residues. These cells failed to grow in the absence of methionine, while cells transformed with a plasmid encoding the wild-type enzyme were able to grow. Although it seems likely that K47 is important for catalytic activity, precedence for a nucleophilic lysine residue does not exist in the acyltransferase literature. In addition, the primary argument posited by Rosen et al. against a nucleophilic cysteine is that C142 is not absolutely conserved since it is not present in the sequence from *Bacillus halodurans*. A sequence alignment of the known HTS sequences demonstrated that this residue is absolutely conserved and that it is present in the *B. halodurans* sequence (a limited alignment is included as Supporting Information, Figure 1). If lysine-47 is not acting as the catalytic nucleophile, the isolation of a succinylated enzyme must be explained in some other manner. One can envision that, under the proper conditions, succinate could travel from cysteine to lysine, even though these residues are located some distance from each other (see below), to form a succinylated-lysine product. The transfer potential from a thioester to an amide is quite large (~6–7 kcal/mol) and would favor formation of the amide. This prompted a closer look at the role of K46 and K47.

Both residues were mutated singly to arginine and to alanine, and the mutants were purified and analyzed for activity. All four mutants had reduced activity in comparison to the wild-type enzyme, with the greatest changes occurring with the K47R and the K47A mutants. Differences were seen in the k_{cat} values and in the K_{M} values for homoserine; the K_{M} value for succinyl-CoA was unchanged with each mutant and indicates that this residue is not important for binding of this substrate. A complete loss of activity would be expected with the alanine mutants if either of the lysine residues were acting as the catalytic nucleophile, and significant reductions in activity would be expected with the arginine mutants. Since K46 is not highly conserved among HTS-like enzymes, it is reasonable to assume that this residue does not directly participate in catalysis. A more likely explanation for the decrease in activity seen with the K46A and K46R mutants is that these substitutions result in small but significant changes in structure that are translated to the active site.

Major decreases in activity were seen with the K47 mutants. This residue is highly conserved among HTS-like sequences, occurring in 88 of 100 aligned sequences. Natural substitutions for this amino acid include glycine (7), alanine (3), and arginine (2); all of the enzymes with the glycine substitution contain lysine at the following position, while no lysine residues are nearby in the alanine-substituted sequences. In general, lysine residues are more likely to participate in catalysis by orienting substrates and modulating basicity (30, 31) or by acting as a general base (32, 33) than by acting as a transient nucleophile (34). They are often acylated, however (35, 36). An examination of the data in Table 1 reveals that, although mutations to lysine-47 result in a lowered k_{cat} value, the V/K for homoserine is basically unaffected. This indicates that lysine-47 plays a role in the first half reaction in this enzyme. The role of K47 was further examined by determining pH profiles for the K47R mutant. The pH profiles for the wild-type enzyme indicate a loss of activity at lower pH values when V_{max} , $V/K_{\text{succ-CoA}}$, and

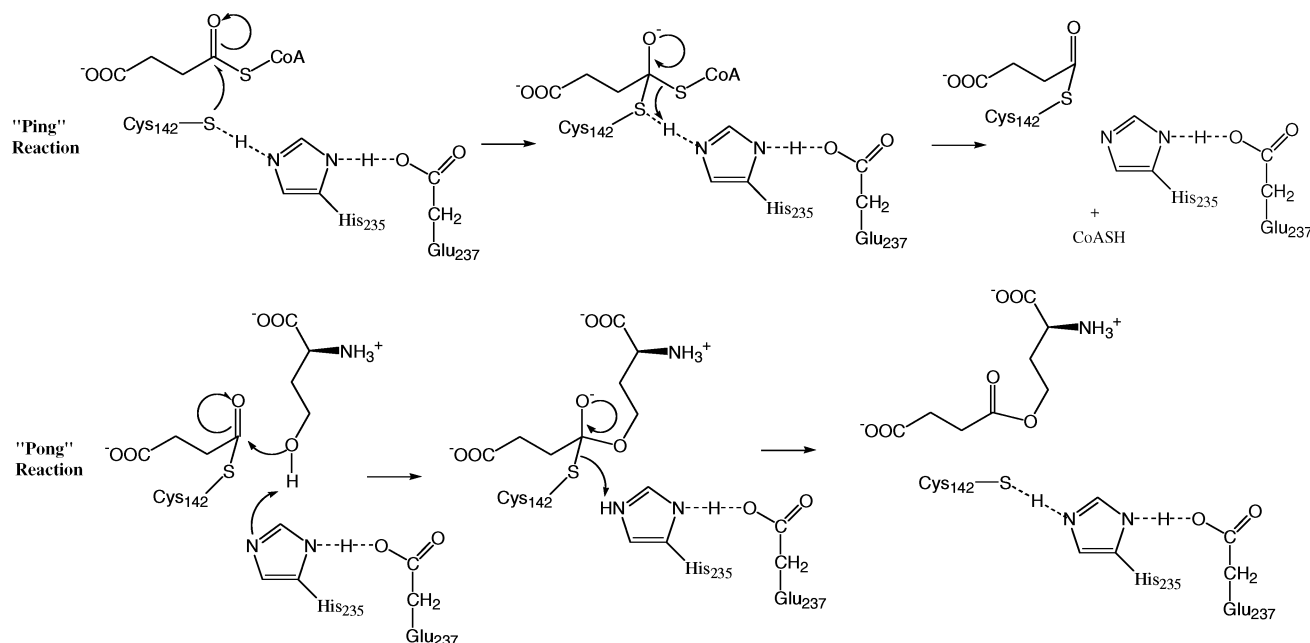


FIGURE 5: Proposed mechanism for transfer of succinate from succinyl-CoA to homoserine as catalyzed by EcHTS. See the text for a detailed description of the proposed mechanism.

$V/K_{\text{homoserine}}$ are examined (8), while the K47R mutant shows a similar trend only in the V_{max} and $V/K_{\text{succ-CoA}}$ profiles. Activity could not be examined at higher pH values due to buffer interference with the assays. The K46A mutant has similar kinetic parameters to the K47R mutant, so its pH dependence was examined to determine if the results obtained with K47R were specific for mutations at that residue. The K46A mutant had a decrease in activity at lower pH when $V/K_{\text{homoserine}}$ was examined, suggesting that the flat pH profile only occurs with K47 substitutions. The flat pH profile for $V/K_{\text{homoserine}}$ at lower pH likely occurs because of the overall reduction in the enzyme catalytic rate. In the wild-type enzyme, protonation of a key residue in the second half reaction resulted in a lowered value of V/K due to a decrease in the rate of this half reaction which was seen as a lowering of the overall enzymatic reaction rate. Although this same protonation presumably occurs in the K47R mutant, the decrease in activity it causes in the second half reaction is not sufficient to lower the overall reaction rate. Hence, this protonation is not observed in the pH profile of the K47R mutant.

Further evidence that K47 plays a role in the first half reaction comes from the pK_a values determined from the V_{max} and $V/K_{\text{succ-CoA}}$ pH profiles with the K47R mutant. The value of 7.5 obtained from both plots is higher than corresponding values of 6.6 and 6.7 obtained with the wild-type enzyme (8). The increase in pK_a suggests that K47 is involved in lowering the ionization constant of the observed residue, ensuring that it will be deprotonated at physiological pH. The affected residue is unknown, but one possibility is the catalytic cysteine. To test this hypothesis, the pH dependence of IAA inactivation was determined for the K47R mutant. If K47 reduces the pK_a of C142, then the IAA inactivation curve should yield a pK_a value of roughly 7.5. Since the observed value of 6.8 is more similar to what is seen with the wild-type enzyme (6.4), K47 does not appear to be directly affecting C142 and may be interacting with some

other residue to indirectly affect the active site or may be interacting with the substrate itself.

These enzymatic data for K47 are consistent with the homology model of EcHTS developed during this study (see Figure 4 and the discussion below). We modeled K47 based on the C α positions of the same residue in TmHTS and BcHTS. The backbone trajectories of the experimental models clearly indicate that the modeled K47 side chain should point away from the main active site residues. There are insufficient structural data to determine what role, if any, K47 may play in substrate recognition, positioning, or release. It is possible that it plays an indirect, yet significant, role in these aspects of catalysis by modulating enzyme conformation rather than directly contacting substrates. We are actively exploring these hypotheses with targeted mutagenesis and structural biology efforts.

The crystal structures of HTS from *B. cereus* and *T. maritima* were recently solved by the Joint Center for Structural Genomics, and their coordinates were deposited in the Protein Data Bank (PDB IDs 2GHR and 2H2W, respectively). These proteins possess 55% sequence identity, and their core structures (239 atoms in each) align with a 0.78 Å rmsd, indicating strong structural similarity. These two experimental structures were used to produce a comparative model of EcHTS (Figure 4). Given the high level of sequence similarity among the three proteins, the BcHTS structure was used to model the majority of EcHTS except for residues corresponding to BcHTS 74 through 84, where the TmHTS model was used as a guide. This region of BcHTS is not present in the deposited structure, indicating that it was extremely flexible and present in numerous conformations. The corresponding region of TmHTS (Figure 4b) has high C α B-factors, implying high mobility. This mobile segment packs against and above the top of helix 2, which contains the key residues K46 and K47.

It is apparent in our model that C142 and H235 are proximal and in a proper orientation and distance for

interaction and hydrogen bonding (Figure 4C). A third amino acid, E237, is found on the opposite side of H235 from C142, and the three amino acids form a structure highly suggestive of a catalytic triad. The arrangement of these residues is similar to other catalytic triad enzymes, such as homoserine transacetylase (37), and these three residues are universally conserved in the HTS family. Again, our model and the two experimental structures are consistent with the involvement of C142 and H235 in catalysis, specifically in their roles of catalytic nucleophile and a stabilizing general base, and strongly suggest local localization of the active site at this position within the enzyme.

Data from our kinetic studies clearly reveal that the K47R and K47A mutants have significantly reduced rates of catalysis. Interestingly, K47 is predicted to be at the beginning of a surface-exposed helix distal from the active site cysteine residue. This position appears inconsistent with K47 being an active site catalytic residue and appears to rule out direct involvement in catalysis. Despite this location, it is possible that K47 controls a conformational change required for transfer of succinate to the enzyme. A second possibility is that K47 is required to hold the succinylated-enzyme intermediate in proper orientation for release of CoA. A third role for this residue is to act as a hinge or shear point, facilitating movement of the helix and opening of the active site for homoserine binding. Despite the extensive kinetic characterization and the experimental structures of two homologous HTS enzymes, it is not possible to clearly distinguish among these possibilities, although an effect on chemistry is more likely than an effect on homoserine binding.

The information now available permits the proposal of a more detailed mechanism for EcHTS (Figure 5). In the first half reaction, succinyl-CoA binds to the enzyme and a covalent bond is formed between the side chain of C142 and the succinyl-CoA thioester. Attack by C142 is facilitated by H235, which acts as a general base to deprotonate the sulfhydryl and form the thiolate anion, and by E237, which stabilizes the protonated form of H235. This results in a tetrahedral intermediate, which breaks down to form the succinylated enzyme and releases CoASH. Protonation of the leaving group by H235, as shown in Figure 5, would assist in breakdown of the intermediate, but no evidence currently exists for this transfer. Lysine-47 plays an undetermined role during this sequence in catalysis, possibly by regulating a conformational change.

In the second half reaction, homoserine binds to the succinylated enzyme and is deprotonated by an active site base. It is possible that H235 fills this role, but this is purely speculative. Homoserine then attacks the succinylated enzyme to form a tetrahedral intermediate. The resulting intermediate would break down to form *O*-succinylhomoserine and regenerate the active enzyme. Again, it is tempting to postulate that H235 facilitates this breakdown by donating a proton to C142. The role of K47 is undefined in the proposed mechanism and additional kinetic experiments and structural data will be required to clarify its role in catalysis.

ACKNOWLEDGMENT

The authors would like to acknowledge Anastasia Midkiff for assistance with the DEPC experiments and the reviewers

for help in the correct interpretation of the lysine mutant data.

SUPPORTING INFORMATION AVAILABLE

An alignment of 17 representative HTS sequences. This alignment highlights the conserved nature of lysine-47, cysteine-142, and histidine-235. This material is available free of charge via the Internet at <http://pubs.acs.org>.

REFERENCES

1. Flavin, M. (1975) Methionine Biosynthesis, in *Metabolic Pathways*, Vol 7, Greenberg, D. M., Ed., Academic, New York.
2. Fuqua, W. C., Winans, S. C., and Greenberg, E. P. (1996) Census and consensus in bacterial ecosystems: the LuxR-LuxI family of quorum-sensing transcriptional regulators, *Annu. Rev. Microbiol.* 50, 727–751.
3. Aitken, S. M., and Kirsch, J. F. (2005) The enzymology of cystathionine biosynthesis: strategies for the control of substrate and reaction specificity, *Arch. Biochem. Biophys.* 433, 166–175.
4. Fowler, B. (2001) The folate cycle and disease in humans, *Kidney Int. Suppl.* 8, S221–229.
5. Nagai, S., and Flavin, M. (1967) Acetylhomoserine: An intermediate in the fungal biosynthesis of methionine, *J. Biol. Chem.* 24, 3884–3895.
6. Saint-Girons, E., Parsot, C., Zakin, M. M., Barzu, O., and Cohen, G. N. (1988) Methionine biosynthesis in *Enterobacteriaceae*: Biochemical, regulatory, and evolutionary aspects, *CRC Crit. Rev. Biochem.* 23, S1–S42.
7. Scheaffer, A. L., Val, D. L., Hanzelka, B. L., Cronan, J. E., and Greenberg, E. P. (1996) Generation of cell-to-cell signals in quorum sensing: Acyl homoserine lactone synthase activity of a purified *Vibrio fischeri* LuxI protein, *Proc. Natl. Acad. Sci. U.S.A.* 93, 9505–9509.
8. Born, T. L., and Blanchard, J. S. (1999) Enzyme-catalyzed acylation of homoserine: Mechanistic characterization of the *Escherichia coli* *metA*-encoded homoserine transsuccinylase, *Biochemistry* 38, 14416–14423.
9. Rosen, R., Becher, D., Büttner, K., Biran, D., Hecker, M., and Ron, E. Z. (2004) Probing the active site of homoserine transsuccinylase, *FEBS Lett.* 577, 386–392.
10. Marti-Renom, M. A., Stuart, A., Fiser, A., Sánchez, R., Melo, F., and Sali, A. (2000) Comparative protein structure modeling of genes and genomes, *Annu. Rev. Biophys. Biomol. Struct.* 29, 291–325.
11. Sali, A., and Blundell, T. L. (1993) Comparative protein modeling by satisfaction of spatial restraints, *J. Mol. Biol.* 234, 779–815.
12. Fiser, A., Do, R. K., and Sali, A. (2000) Modeling of loops in protein structures, *Protein Sci.* 9, 753–1773.
13. DeLano, W. L. (2002) The PyMOL Molecular Graphics System, DeLano Scientific, San Carlos, CA.
14. Polgar, L. (1974) Mercaptide-imidazolium ion-pair: the reactive nucleophile in papain catalysis, *FEBS Lett.* 47, 15–18.
15. Wang, J., Vath, G. M., Gleason, K. J., Hanna, P. E., and Wagner, C. R. (2004) Probing the mechanism of hamster arylamine N-acetyltransferase 2 acetylation by active site modification, site-directed mutagenesis, and pre-steady state and steady state kinetic studies, *Biochemistry* 43, 8234–8246.
16. Sarkany, Z., Skern, T., and Polgar, L. (2000) Characterization of the active site thiol group of rhinovirus 2A proteinase, *FEBS Lett.* 481, 289–292.
17. Mares, R., Urbanowski, M. L., and Stauffer, G. V. (1992) Regulation of the *Salmonella typhimurium* *metA* gene by the MetR protein and homocysteine, *J. Bacteriol.* 174, 390–397.
18. Ron, E. Z., and Shani, M. (1971) Growth rate of *Escherichia coli* at elevated temperatures: Reversible inhibition of homoserine trans-succinylase, *J. Bacteriol.* 107, 397–400.
19. Biran, D., Brot, N., Weissbach, H., and Ron, E. Z. (1995) Heat shock-dependent transcriptional activation of the *metA* gene of *Escherichia coli*, *J. Bacteriol.* 177, 1374–1379.
20. Lee, L.-W., Ravel, J. M., and Shive, W. (1966) Multimetalite control of a biosynthetic pathway by sequential metabolites, *J. Biol. Chem.* 241, 5479–5480.
21. Brush, A., and Paulus, H. (1971) The enzymatic formation of *O*-acetylhomoserine in *Bacillus subtilis* and its regulation by

- methionine and S-adenosylmethionine, *Biochem. Biophys. Res. Commun.* 45, 735–741.
22. Bazan, J. F., and Fletterick, R. J. (1988) Viral cysteine proteases are homologous to the trypsin-like family of serine proteases: structural and functional implications, *Proc. Natl. Acad. Sci. U.S.A.* 85, 7872–7876.
23. Sfakianos, M. K., Wilson, L., Sakalian, M., Falany, C. N., and Barnes, S. (2002) Conserved residues in the putative catalytic triad of human bile acid coenzyme A:amino acid N-acyltransferase, *J. Biol. Chem.* 277, 47270–47275.
24. Davis, J. P., Zhou, M. M., and Van Etten, R. L. (1994) Kinetic and site-directed mutagenesis studies of the cysteine residues of bovine low molecular weight phosphotyrosyl protein phosphatase, *J. Biol. Chem.* 269, 8734–8740.
25. Chen, L., MacMillan, A. M., Chang, W., Ezaz-Nikpay, K., Lane, W. S., and Verdine, G. L. (1991) Direct identification of the active-site nucleophile in a DNA (cytosine-5)-methyltransferase, *Biochemistry* 30, 11018–11025.
26. Sarkany, Z., and Polgar, L. (2003) The unusual catalytic triad of poliovirus protease 3C, *Biochemistry* 42, 516–522.
27. Jia, Y., Kappock, T. J., Frick, T., Sinskey, A. J., and Stubbe, J. (2000) Lipases provide a new mechanistic model for polyhydroxybutyrate (PHB) synthases: characterization of the functional residues in *Chromatium vinosum* PHB synthase, *Biochemistry* 39, 3927–3936.
28. Tseng, C. C., McLoughlin, S. M., Kelleher, N. L., and Walsh, C. T. (2004) Role of the active site cysteine of DpgA, a bacterial type III polyketide synthase, *Biochemistry* 43, 970–980.
29. Miles, E. W. (1977) Modification of histidyl residues in proteins by diethylpyrocarbonate, *Methods Enzymol.* 47, 431–442.
30. Gruber, K., Gartner, G., Krammer, B., Schwab, H., and Kratky, C. (2004) Reaction mechanism of hydroxynitrile lyases of the α/β -hydrolase superfamily, *J. Biol. Chem.* 279, 20501–20510.
31. Patridge, K. A., Weber, C. H., Friesen, J. A., Sanker, S., Kent, C., and Ludwig, M. L. (2003) Glycerol-3-phosphate cytidylyl-transferase: Structural changes induced by binding of CDP-glycerol and the role of lysine residues in catalysis, *J. Biol. Chem.* 278, 51863–51871.
32. Karsten, W. E., Liu, D., Jagannatha, G. S., Harris, B. G., and Cook, P. F. (2005) A catalytic triad is responsible for acid-base chemistry in the *Ascaris serum* NAD-malic enzyme, *Biochemistry* 44, 3626–3635.
33. Feldman, A. R., Lee, J., Delmas, B., and Paetzel, M. (2006) Crystal structure of a novel viral protease with a serine/lysine catalytic dyad mechanism, *J. Mol. Biol.* 358, 1378–1389.
34. He, Z., and Toney, M. D. (2006) Direct detection and kinetic analysis of covalent intermediate formation in the 4-amino-4-deoxychorismate synthase catalyzed reaction, *Biochemistry* 45, 5019–5028.
35. Peterson, C. L., and Laniel, M. A. (2004) Histones and histone modifications, *Curr. Biol.* 14, R546–51.
36. Polevoda, B., and Sherman, F. (2002) The diversity of acetylated proteins, *Genome Biol.* 3, 1–6.
37. Mirza, I. A., Nazi, I., Korczynska, M., Wright, G. D., and Berghuis, A. M. (2005) Crystal structure of homoserine transacetylase from *Haemophilus influenzae* reveals a new family of α/β -hydrolases, *Biochemistry* 44, 15768–15773.

BI0620252